Journal of Catalysis **202,** 413–420 (2001)
doi:10.1006/jcat.2001.3301, available online at http://www.idealibrary.com on IDEAL®

Fourier Transform Infrared Study of the Performance of Nanostructured TiO_2 Particles for the Photocatalytic Oxidation of Gaseous Toluene

A. J. Maira,*,[1] J. M. Coronado,* V. Augugliaro,† K. L. Yeung,‡ J. C. Conesa,* and J. Soria*

*Instituto de Catálisis y Petroleoquímica, CSIC, Campus Cantoblanco, 29049 Madrid, Spain; †Dipartimento di Ingegneria Chimica dei Processi e dei Materiali, Università di Palermo, Viale delle Scienze, 90128 Palermo, Italy; and ‡Department of Chemical Engineering, The Hong Kong University of Science and Technology, Clear Water Bay, Kowloon, Hong Kong

Received April 6, 2001; revised May 31, 2001; accepted May 31, 2001

Thermal and hydrothermal treatments have been applied to an amorphous TiO_2 precursor for obtaining nanosized TiO_2 particles (P11t and P11h, respectively) of different photocatalytic properties. The activity of these catalysts has been tested by performing the toluene oxidation in gas phase in a continuous photoreactor. A Fourier transform infrared (FTIR) investigation of the catalysts under conditions prevailing during the test photoreaction has also been carried out. The photoreactivity results showed that CO_2 was the main oxidation product and benzaldehyde a stable intermediate. Anatase P11t photoactivity was similar to that observed for commercial photocatalysts, while anatase P11h presented a marked improvement. The FTIR study on these samples indicate that P11h has a higher number of hydrogen-bonded hydroxyl groups that are more stable under RT outgassing than P11t. The higher photoactivity of P11h is attributed to the participation of these hydrogen-bonded hydroxyls in the toluene conversion to CO_2. FTIR spectra also suggest that benzaldehyde, the minor oxidation product, originates from toluene adsorbed on isolated hydroxyls. Benzaldehyde is more strongly adsorbed on P11h than on P11t; the presence of water vapor in the reacting mixture, however, facilitates its desorption and/or photooxidation.

Key Words: **photocatalysis; nanoparticles; titanium dioxide; toluene; volatile organic compounds; FTIR; hydrothermal treatment.**

1. INTRODUCTION

Heterogeneous photocatalytic oxidation (PCO) is a promising technology for degradation of volatile organic compounds (VOCs) in process air streams (1–3). This technology is capable of oxidizing airborne VOCs into CO_2, H_2O, and mineral compounds (e.g., HX, where X = Cl, Br) at room temperature utilizing a semiconductor catalyst (e.g., TiO_2) and a UV or near-UV light source. When the catalyst absorbs photons having energy greater than the band gap of the semiconductor, electrons are excited from the valence to the conduction band leaving holes behind. The resulting electron–hole pairs can migrate toward the catalyst surface and initiate redox reactions that oxidize the adsorbed organic molecules. However, reduced quantum yields, along with the possible generation of undesirable byproducts, are the main limiting factors of this technology (4). Catalyst deactivation is also a problem for PCO of certain pollutants (e.g., aromatic compounds). Different approaches have been adopted to overcome some of these limitations, including reactor design improvement (5) and photocatalyst modification (6–10).

Recent reports have shown that nanostructured anatase-TiO_2 particles exhibited higher activity (6–8) and selectivity (8) than the commercial TiO_2 (P25, Degussa) for the gas-phase PCO of VOC. The nanostructured TiO_2 provides a larger surface area for adsorption and decomposition of VOC. Quantum size effects were also observed for the nanometer-sized TiO_2 particles (7, 10). A shift in the semiconductor bandgap to higher energies was observed when the TiO_2 particle size was decreased, resulting in lower photon utilization. The photogenerated e^-/h^+ pairs also exhibit different reactivity, depending on the TiO_2 particle size and redox potential of the adsorbed molecules. As the particle size diminishes, the structure of the TiO_2 catalyst undergoes changes resulting in a redistribution of the planar, edge, and corner sites. These structural changes are expected to affect the activity of the photocatalyst. However, the TiO_2 surface structure is probably affected not only by the particle size but also by the TiO_2 preparation method. The surface hydroxyl groups have been recognized to play an important role in the photodegradation process through their interactions with photogenerated holes (1, 11, 12), and the preparation method could affect the hydroxylation state of the catalyst surface.

In this paper TiO_2 samples with the same particle size (11 nm) were prepared from an amorphous precursor by thermal and hydrothermal methods. It is expected that the crystallization of anatase TiO_2 under hydrothermal conditions will create a different hydrated surface from that of conventional thermal treatment. The photocatalytic activity of these catalysts was investigated for the gas-phase

[1] To whom correspondence should be addressed. Fax: 34-91 5854760. E-mail: jmaira@icp.csic.es.

0021-9517/01 $35.00

photooxidation of toluene. A comparative IR study of the surface structure of these two samples was also conducted under reaction conditions in an *in situ* IR cell.

2. EXPERIMENTAL

2.1. Catalyst Preparation and Characterization

Titanium isopropoxide (TIP) was used as the precursor for the sol–gel synthesis of nanostructured TiO_2 catalysts. The synthesis was conducted by controlled addition of 1 ml of TIP into a well-mixed isopropanol–water solution under N_2 atmosphere. After the addition, the mixture was aged for 1 h at room temperature. The titania powder was recovered by filtration and dried in an oven at 338 K for 24 h. The resulting amorphous titania was then transformed into crystalline TiO_2 particles using two different treatment procedures: thermal and hydrothermal methods. For the thermal treatment, the amorphous titania powder was placed in a high-temperature furnace and calcined in air at 723 K for 3 h. In the second method, the amorphous TiO_2 powder ($\sim$0.2 g) was mixed with 2.5 ml of H_2O and 25 ml of ethanol into a 150-ml, Teflon-lined autoclave vessel (PTFE-4748, Parr Scientific). The vessel was then placed in a preheated, air-convection oven (Memmert, UE200-220C-SS) set at 473 K for 8 h. Anatase-TiO_2 powder was crystallized under the hydrothermal action of the alcohol–water solution. The powder was recovered by centrifugation, rinsed with deionized distilled water, and dried in an oven at 338 K for 24 h. For both preparation methods, the size of the TiO_2 particle can be controlled through the treatment condition (7). In this work, these conditions were chosen to obtain a TiO_2 crystal size of 11 nm; hereafter the catalysts prepared by thermal and hydrothermal treatments are referred to as P11t and P11h, respectively.

The crystal structure, particle size, and surface area of the TiO_2 photocatalysts were determined using X-ray diffraction (XRD) and nitrogen physi-adsorption. The TiO_2 powders were analyzed by XRD using a Philips PW 1030 X-ray diffractometer equipped with a Cu$K\alpha$ radiation source and a graphite monochromator. The BET surface area of the TiO_2 was measured by nitrogen physi-adsorption (Micromeritics ASAP 2010). The UV–vis adsorption spectra of the TiO_2 catalysts were measured using a Shimadzu UV-2100 spectrophotometer.

2.2. Photoreactor Setup

The details of the experimental setup and photoreactor used for the gas-phase photooxidation of toluene have been published elsewhere (8). The experimental setup consists of three main units: (i) the gas and vapor feed delivery module, (ii) the photoreactor, and (iii) the analytical system. The toluene vapor feed was obtained by metering liquid toluene (Panreac, PAI) using a syringe pump (kdScientific 1000) to a constant temperature heat exchanger. The vaporized toluene was mixed with wet oxygen before entering the photoreactor. Water was added by bubbling the dry O_2 gas through a saturator containing distilled water at 298 K. For all the runs, the water content of the reacting mixture was kept constant at 2.5×10^{-2} molar fraction. The flow rate of oxygen was adjusted using a calibrated flow meter.

The activity and selectivity of the catalyst for PCO of toluene were tested in a continuous flow annular photoreactor. The reactor was made of two concentric Pyrex tubes of 200-mm length. The 100 mg of catalyst was coated onto the central section (L = 150 mm) of the inner tube (outer diameter = 16 mm) from a concentrated suspension of TiO_2 nanoparticles. After a day of ambient drying, the catalyst forms a uniform layer that exhibits good adhesion to the glass support. The reactant gas flows through the narrow annular gap (1 mm thickness) formed between the two glass tubes. The catalyst was irradiated by four 210-mm-long fluorescent black lamps (6 W, Sylvania, 6WBLB-T5), symmetrically positioned outside the photoreactor. Both photoreactor and lamps were enclosed in a box covered internally with reflective aluminum foil. The composition of the outlet gas was analyzed using an on-line gas chromatograph (HP G1800C) equipped with a HP5 capillary column (0.25 mm inner diameter $\times$ 30 m) and an electron ionization detector.

The PCO runs of toluene were conducted at 343 K and atmospheric pressure. In a typical experiment, the reacting mixture was fed to the photoreactor for about 1 h before UV irradiation. During this period, the toluene concentration was monitored until a steady-state condition was reached. This provides the inlet concentration of toluene. The UV lamps were then switched on and the outlet concentration was measured continuously with time. The reaction rate and conversion values were calculated from the inlet and outlet toluene concentrations, while the selectivity was based on the amounts of CO_2 and benzaldehyde, the only toluene oxidation products detected in the effluent. All the experiments were carried out at a fixed flow rate of 7.5×10^{-5} mol s^{-1} and an inlet toluene concentration of 0.06 mM (i.e., 1200 ppmv). The mean residence time of gas inside the tube connecting the photoreactor with the gas chromatograph was about 4 s.

2.3. Fourier Transform Infrared (FTIR) Measurements

For the Infrared (IR) experiments, a Nicolet 5ZDX FTIR spectrometer equipped with a MCT detector (4 cm^{-1} resolution) was used. The TiO_2 powder was pressed into a thin wafer (25 mg cm^{-2}) and placed in an IR Pyrex cell equipped with NaCl windows. The cell can be evacuated by connecting to a conventional vacuum line (residual pressure: 1×10^{-4} Torr). Measured amounts of reactants (i.e., toluene and oxygen) can be metered to the reactor

cell. For irradiating the wafer, the IR cell was introduced into the same box used for performing the photoreactivity tests.

The IR spectra of both samples were recorded after the following treatments performed at room temperature: (i) evacuation for 15 min, (ii) evacuation for 2 h, (iii) introduction of 5 Torr of toluene (Panreac, PAI) into the IR cell and subsequent introduction of 50 Torr of oxygen; (iv) irradiation for 30 min, (v) evacuation of the sample for 15 min, (vi) introduction of 5 Torr of H_2O into the cell, and (vii) irradiation for 30 min. Toluene and water were previously distilled in vacuum.

3. RESULTS

3.1. Catalyst Characterization

X-ray diffraction analyses indicated that the two TiO_2 catalysts prepared by thermal and hydrothermal methods were anatase, with a crystal size of 11 nm. Both samples also have comparable BET surface areas, as measured by nitrogen physisorption. Table 1 gives the details of the treatment conditions, primary particle size, and BET surface area of two TiO_2 catalysts. Since the same UV–vis adsorption spectra were obtained for both catalysts, the band gap was not affected by the preparation method, as expected for samples with the same particle size (7, 10).

3.2. Toluene Photocatalytic Oxidation

The toluene photooxidation products detected in the gas phase were CO_2 and benzaldehyde. The absence of other intermediates was also confirmed by the carbon mass balance that was satisfactorily fulfilled by CO_2 and benzaldehyde during the course of all the runs. Figure 1A plots the toluene degradation rates per unit of surface area (r_1) and the toluene conversion values for P11h and P11t catalysts as a function of time on-stream. Figure 1B displays the benzaldehyde production rates per unit of surface area (r_2) over both catalysts as a function of irradiation time. By starting from a high conversion value, the P11t catalyst undergoes a fast deactivation process to reach steady-state conditions characterized by a relatively low conversion value.

TABLE 1

Preparation Method and Conditions, Primary Particle Size, and Surface Area of TiO_2 Catalysts

Catalyst	Treatment	Conditions Temperature/ water	Primary particle size (nm)[a]	Surface area (m^2/g)
P11h	Hydrothermal	473 K/2.5 ml H_2O	11	95
P11t	Thermal	723 K for 3 h	11	96

[a] Primary particle size measured from XRD line broadening.

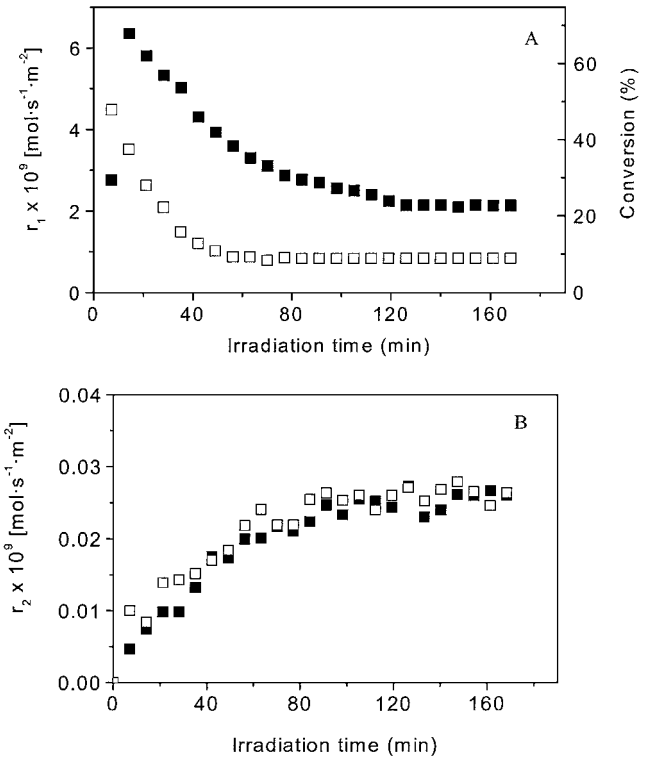

FIG. 1. Toluene degradation rate, r_1, and toluene conversion (A) and benzaldehyde formation rate r_2(B) versus irradiation time for P11h (■) and P11t (□) TiO_2, using an oxygen flow rate of 7.5×10^{-5} mol s^{-1} and an initial toluene concentration of 0.06 mM.

This pattern of activity may be repeated only after a catalyst rehydroxylation process; otherwise the maximum is not observed. In comparison with P11t, the toluene conversion on P11h catalyst exhibits a slower increase, followed by a softer deactivation process. Figure 1A shows that both the maximum and steady-state conversion values of P11h catalyst are higher than those of P11t. This indicates that the hydrothermally treated catalyst is more active for the toluene photooxidation than the thermally treated one. From the r_2 data reported in Fig. 1B, the benzaldehyde production rate increases with irradiation time until a steady-state value is reached; the duration of this increase roughly corresponds to that of the transient state of the catalysts. When the toluene steady conversion was reached, the selectivity for benzaldehyde was 6% for P11t and 1.5% for P11h. Although the toluene conversion rate of P11h is nearly three times higher than that of P11t, the benzaldehyde production rates of the two catalysts are comparable. The toluene degradation rate obtained in the steady state for the commercial TiO_2 P25 (Degussa), 0.9×10^{-9} mol s^{-1} m^{-2}, was similar to that observed for P11t.

3.3. FTIR Spectra

3.3.1. P11t sample. The FTIR spectrum of a hydrated P11t sample outgassed for 15 min at 295 K is presented in

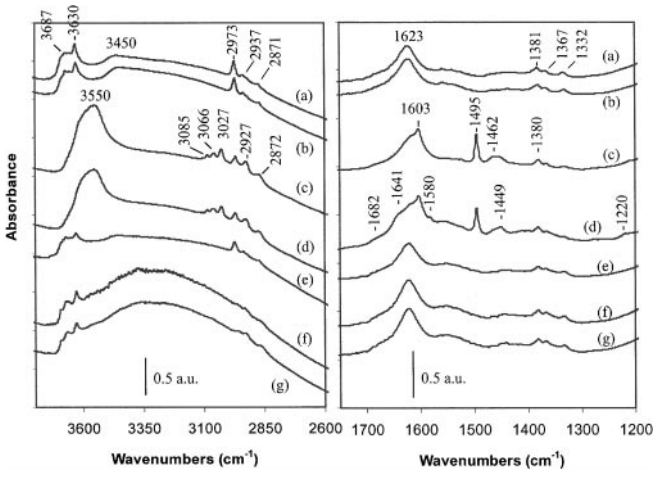

FIG. 2. FTIR spectra of P11t TiO_2 after the following treatments performed at room temperature: (a) evacuation for 15 min, (b) evacuation for 2 h, (c) introduction of 5 Torr of toluene into the IR cell and subsequent introduction of 50 Torr of oxygen, (d) irradiation for 30 min, (e) evacuation of the sample for 15 min, (f) introduction of 5 Torr of H_2O into the cell, and (g) irradiation for 30 min.

Fig. 2a. This spectrum shows a narrow band at 3630 cm^{-1}, which is accompanied by weak shoulders at 3674 and 3687 cm^{-1}, due to the (ν_{OH}) mode of different types of isolated hydroxyl groups (13–15). The broad IR absorption in the 3600–2800 cm^{-1} range, with a maximum at 3450 cm^{-1}, arises from the superposition of the ν_{OH} mode of interacting hydroxyl groups (i.e., involved in hydrogen bonds) and the symmetric and antisymmetric ν_{OH} modes of molecular water coordinated to Ti^{4+} cations (13, 16). The band at 1623 cm^{-1} is assigned to the molecular water bending mode, while the narrow bands at 2973, 2937, 2871, 1381, 1367, and 1332 cm^{-1} are due to organic residues originating from the sample as a result of the preparation procedure. The effect of this short outgassing treatment on the spectrum of the fresh sample (spectrum similar to Fig. 2f) was mainly an important decrease of the broad absorption in the 3600–2500 cm^{-1} range and of the band at 1640 cm^{-1}, indicating the removal of a large part of weakly adsorbed water. A subsequent outgassing of the sample for 2 h (Fig. 2b) produces a small decrease of the isolated hydroxyl bands. The observation of this small modification indicates that the removal of most of the weakly adsorbed water and interacting hydroxyls has taken place during the first outgassing treatment.

Upon toluene adsorption, the narrow bands of the isolated hydroxyl groups are replaced by a broad band centered at 3550 cm^{-1} (Fig. 2c). In addition, a small decrease in the intensity of the broad absorption, as well as in the 1623 cm^{-1} band, is observed. These results indicate that toluene adsorption takes place mainly on isolated hydroxyls at the P11t surface, their interaction yielding the new band at 3550 cm^{-1}. Toluene may also displace some adsorbed water molecules, as indicated by the minimum observed at 1623 cm^{-1} in the spectrum shown in Fig. 3b. This figure, obtained by subtracting spectrum 2b from spectrum 2c, also shows the formation of narrow bands at 3085, 3066, 3027, 2927, 2872, 1603, 1495, 1460, and 1380 cm^{-1}. The bands observed in the 3100–2850 cm^{-1} range have been assigned to $\nu_{C\text{-}H}$ of the aromatic ring (3085, 3066, and 3027 cm^{-1}) and to asymmetric and symmetric $\nu_{C\text{-}H}$ of the methyl group (2927 and 2872 cm^{-1}, respectively) (17). The bands at 1603 and 1495 cm^{-1} have been assigned to the in-plane skeletal vibrations of aromatic rings, and the bands at 1460 and 1380 cm^{-1} have been associated with the asymmetric and symmetric CH_3 bending vibrations, respectively (17).

The subsequent irradiation of the sample (Fig. 2d) caused a small decrease in the 3550 cm^{-1} band and a slight increase in the broad bands positioned at the 3500–3000 cm^{-1} range. The irradiation also led to a small decrease of the narrow bands due to adsorbed toluene (the irradiation was carried out with toluene in the gas phase; Fig. 3c) and the formation of several small bands in the 1900–1100 cm^{-1} range (1682, 1641, 1595, 1580, 1449, 1350, and 1220 cm^{-1}). Similar bands have been reported for benzaldehyde adsorption on nanostructured TiO_2 (18) and Degussa TiO_2 P25 (19–21). The band at 1682 cm^{-1} has been assigned to the carbonyl vibration of the aldehyde group, while bands at 1641, 1595, and 1580 cm^{-1} arise from the different vibrational modes of the aromatic ring (18). These results indicate that part of the toluene adsorbed on the isolated hydroxyl group (band at 3550 cm^{-1}) is photooxidized, but the bands corresponding to those adsorption sites are not regenerated well because these hydroxyls were lost during the photoreaction or because they are also acting as adsorption sites for benzaldehyde.

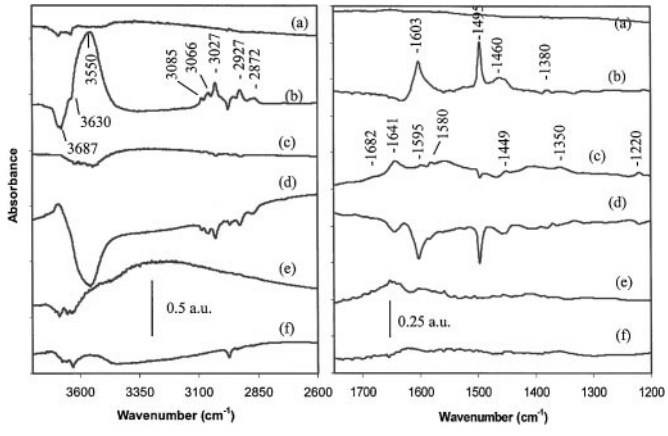

FIG. 3. Effect of (a) evacuation for 2 h (subtraction of spectrum 2a from spectrum 2b), (b) toluene adsorption (subtraction of spectrum 2b from spectrum 2c), (c) irradiation (subtraction of spectrum 2c from spectrum 2d), (d) subsequent evacuation (subtraction of spectrum 2d from spectrum 2e), (e) water adsorption, and (f) accumulated effects of consecutive toluene adsorption, UV irradiation, and subsequent outgassing at 298 K (subtraction of spectrum 2b from spectrum 2e) for P11t TiO_2.

After a subsequent outgassing at 295 K (Fig. 2e) the 3550 cm^{-1} band practically disappears and the bands of isolated hydroxyls are partially recovered. These two observations, together with the disappearance of the adsorbed toluene bands at 3085, 3066, 3027, 2927, 2872, 1603, 1495, 1462, and 1380 cm^{-1}, are coherent with the proposal that toluene was weakly adsorbed on these hydroxyls. The decrease of the narrow bands at 1641, 1595, 1580, 1449, 1350, and 1220 cm^{-1} indicates that, in addition to toluene, a small amount of benzaldehyde is also desorbed. The spectrum shown in Fig. 3f, obtained from subtracting spectrum 2b from spectrum 2e, gives an indication of the modifications produced in the photocatalyst by consecutive treatments of toluene adsorption, UV irradiation, and desorption (i.e., 295 K). These data show that the main result for these treatments is the loss of isolated and interacting hydroxyls on the P11t surface.

By contacting this treated sample with water vapor, the spectrum shown in Fig. 2f was obtained. The similarity to the fresh sample spectrum indicates that the initial surface hydration can be , at least partially, recovered. A subsequent irradiation of the sample gives rise to the spectrum 2g, which only shows a small decrease of the adsorption in the 3600–2800 cm^{-1} range.

3.3.2. P11h sample. The outgassing of the fresh P11h sample (whose FTIR spectrum is similar to Fig. 4f) at 295 K for 15 min produces mainly a decrease of both the broad absorption centered at 3580 cm^{-1} and the 1648 cm^{-1} band. The low stability presented in outgassing treatment by these bands, as in the case of P11t, indicates that they correspond to weakly adsorbed water. The spectrum obtained after that treatment Fig. 4a shows two narrow bands at 3687 and

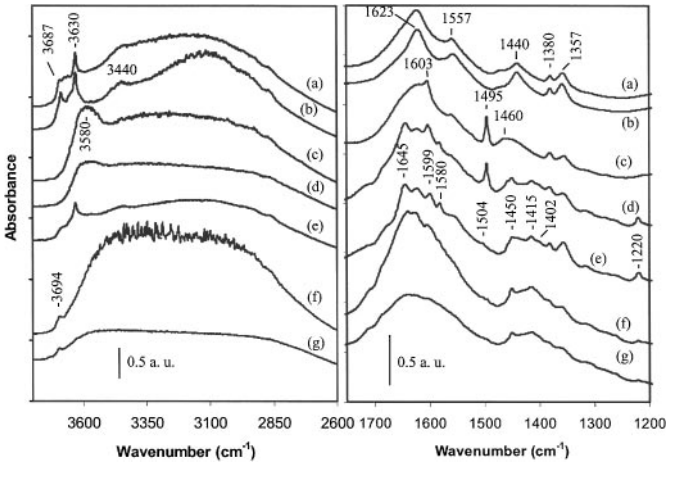

FIG. 4. FTIR spectra of P11h TiO_2 after the following treatments performed at room temperature: (a) evacuation for 15 min, (b) evacuation for 2 h, (c) introduction of 5 Torr of toluene into the IR cell and subsequent introduction of 50 Torr of oxygen, (d) irradiation for 30 min, (e) evacuation of the sample for 15 min, (f) introduction of 5 Torr of H_2O into the cell, and (g) irradiation for 30 min.

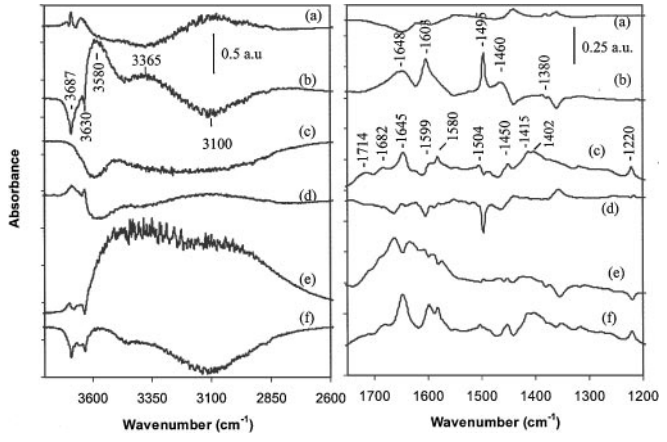

FIG. 5. Effect of (a) evacuation for 2 h (subtraction of spectrum 4a from spectrum 4b), (b) toluene adsorption (subtraction of spectrum 4b from spectrum 4c), (c) irradiation (subtraction of spectrum 4c from spectrum 4d), (d) subsequent evacuation (subtraction of spectrum 4d from spectrum 4e), (e) water adsorption, and (f) accumulated effects of consecutive toluene adsorption, UV irradiation, and subsequent outgassing at 298 K (subtraction of spectrum 4b from spectrum 4e) for P11h TiO_2.

3630 cm^{-1}, with shoulders at 3675 and 3655 cm^{-1}, due to isolated hydroxyl groups; the intensity of those bands is relatively similar to that observed for P11t. The spectrum also shows two broad absorptions in the 3600–2800 cm^{-1} range, the main one centered at 3100 cm^{-1} and the other at 3440 cm^{-1}. Other bands are observed at 1623 cm^{-1}, due to adsorbed water, and at 1557, 1440, 1380, and 1357 cm^{-1}, probably due to organic residues. Thus, the main difference between the spectra obtained for hydrated P11t and P11h samples outgassed for 15 min is the stability of the broad band at 3100 cm^{-1} observed for P11h. A subsequent outgassing of P11h at 295 K for 2 h (Fig. 4b) produces mainly a decrease of the broad absorptions centered at 3580 cm^{-1} and 3360 cm^{-1} and of the shoulder at 1648 cm^{-1}, together with an increase of the broad band centered at 3100 cm^{-1} and the bands corresponding to isolated hydroxyl groups. These effects can be clearly seen in Fig. 5a, obtained by subtracting spectrum 4a from spectrum 4b. As the expected result of the outgassing treatment is the removal of water molecules, the decreasing intensities of bands should correspond to adsorbed water, whereas the increasing bands are due to the water adsorption sites, isolated and H-bonded hydroxyls. Water molecules and H-bonded hydroxyl groups are retained on P11h more strongly than on P11t.

Toluene adsorption on the outgassed P11h sample results in several changes in the spectrum (Fig. 4c) that can be seen more clearly by subtracting the spectrum shown in Fig. 4b from that of Fig. 4c. Figure 5b shows that toluene adsorption results in the disappearance of the isolated hydroxyl bands and the decrease of the broad absorption centered at 3100 cm^{-1}, while broad bands at 3580 and 3365 cm^{-1} are formed. The formation of the band at 3580 cm^{-1} is due to the interaction of isolated hydroxyls with adsorbed toluene.

The formation of the broad band centered at 3365 cm^{-1} and a narrower band at 1647 cm^{-1}, together with the decrease of the 3100 cm^{-1} band, indicates that toluene adsorption on H-bonded hydroxyls originates these new bands. In addition, the adsorbed toluene bands at 1603, 1495 and 1460 cm^{-1} are observed, whereas the bands assigned to organic residues show a decrease, probably due to interactions with adsorbed toluene.

Irradiation of P11h containing toluene for 30 min (Fig. 4d) produces a decrease in the broad absorption bands at 3580 cm^{-1} and in the 3500–2800 cm^{-1} range. The narrow bands attributed to adsorbed toluene molecules display a slight decrease, as observed in the spectrum difference (Fig. 5c), obtained by subtraction of spectrum 4c from spectrum 4d. At the same time, new signals located at 1714, 1682, 1645, 1599, 1580, 1504, 1450, 1415, 1402, and 1220 cm^{-1} were assigned to benzaldehyde adsorbed on the P11h surface, as in the case of P11t. The decrease of the 3580 cm^{-1} band created by toluene adsorbed on isolated hydroxyl groups, without the recovery of the adsorption sites bands, indicates that these isolated hydroxyls have been lost during the photooxidation of the adsorbed toluene. The decrease of the overall broad absorption in the 3450–2800 cm^{-1} range indicates that part of the toluene adsorbed on interacting hydroxyl groups, as well as part of those hydroxyls, has been lost by photooxidation and/or photodesorption. All these hydroxyl species decrease even though water must be produced in the toluene photooxidation process and could lead to an increase in IR adsorption.

A subsequent outgassing of the irradiated P11h sample (Fig. 4e) results in the disappearance of the bands related to toluene adsorption (broad bands at 3580 and 3365 cm^{-1} and narrow bands at 1604, 1495, 1460, and 1380 cm^{-1}). A slight decrease of the adsorbed benzaldehyde bands is also evident. These effects can be clearly seen in Fig. 5d, obtained by subtracting spectrum 4d from spectrum 4e. Toluene desorption from the catalyst surface allows the observation of some isolated hydroxyls that previously were interacting with toluene. That is the case for most of these hydroxyl groups represented by the band at 3680 cm^{-1}. Some of the interacting hydroxyls (broad band at 3100 cm^{-1}) are also observed once toluene is desorbed.

The accumulated effects of consecutive toluene adsorption, UV irradiation, and outgassing at 295 K on the sample surface are summarized in the plot shown in Fig. 5f, obtained by subtracting spectrum 4b from spectrum 4e. The effect is a partial loss of interacting and isolated hydroxyls (particularly those corresponding to the band at 3687 cm^{-1}) and the retention of adsorbed benzaldehyde in a larger amount than in the case of P11t (Fig. 3f).

Exposure of the treated P11h sample to water vapor (Fig. 4f) results in a marked increase of the broad absorption in the 3600–2800 cm^{-1} range, indicating the regeneration of interacting hydroxyl groups and adsorbed water molecules on the sample surface. A significant increase of the IR absorption in the 1750–1500 cm^{-1} range, where the bending vibrations of adsorbed water appear, is evidenced by Fig. 5e obtained by subtracting spectrum 4e from spectrum 4f. This increase and the broadening of the adsorption are accompanied by a decrease of the narrow bands corresponding to benzaldehyde adsorbed on hydroxyl groups and organic residues. At the same time, a small increase of the isolated hydroxyl bands, mainly the one at 3694 cm^{-1}, is observed. These results indicate that by water incorporation, some adsorbed benzaldehyde molecules are released from the adsorption sites but probably remain on the hydrated P11h surface, contributing to part of the 1750–1500 cm^{-1} broad absorption.

Subsequent irradiation of this rehydrated sample (Fig. 4g) results in a decrease of both the broad absorption in the 3600–2800 cm^{-1} range and the 1630 cm^{-1} band, indicating photodesorption of adsorbed water and interacting hydroxyl groups. In addition, a small decrease of the adsorbed benzaldehyde bands and the broad adsorption in the 1750–1500 cm^{-1} range indicates that benzaldehyde photodegradation has also taken place.

4. DISCUSSION

Although P11t and P11h are anatase with a crystal size of 11 nm and very similar surface areas (see Table 1), their photocatalytic properties for toluene degradation under the same experimental conditions show significant differences, which must be due to different bulk and/or surface properties. The bulk properties determine the processes of charge carrier photogeneration and diffusion (22), whereas those of the surface influence both organic molecule adsorption and the generation of species necessary for photoreaction. In the present work, significant correlations are revealed by the comparison of photocatalytic activities and amounts of IR-detected adsorbed species, which point to relevant aspects of the influence of hydroxyl groups in the process, not only through their direct participation in the reaction mechanism (by trapping of charge carriers reaching the catalyst surface to produce very reactive surface OH radicals) but also by affecting the adsorption of reactant molecules: on one hand, hydroxyl groups are known to act as active sites for toluene adsorption (11, 12); on the other hand, they may cover the sites (exposed titanium cations with unsaturated coordination) where electron trapping by adsorbed oxygen takes place; this process is important not only for producing the oxygen radicals active in toluene oxidation but also for hindering electron–hole recombination processes that may limit the number of charge carriers available for the photocatalytic reaction.

The spectroscopic and reaction tests provide some useful information on mechanistic aspects of the process. Of course, because the experimental conditions are not the

same for both types of experiment, the particular conditions of each measurement may need to be taken into account when trying to relate the corresponding results. Thus, different from the conditions imposed during the FTIR studies, in the photoreaction tests the presence of a continuous supply of water vapor in the gas flow should favor a higher surface hydration, which can affect the proportion of isolated and interacting hydroxyls and thus the types and amount of adsorbed toluene, while the continuous removal of products may lead to adsorbed species which are different from those in the IR studies. Still, the basic phenomena should remain the same and clarifications of the process features can be extracted from the comparisons.

Data obtained show that both in the photocatalytic activity and in the FTIR results, P11t and P11h present some similarities in part of the behavior, whereas they differ in others. Thus, the FTIR spectra after toluene adsorption in the dark on the samples outgassed at 298 K indicate that before irradiation toluene is adsorbed on both isolated and H-bonded hydroxyls at the catalyst surfaces (Figs. 2c, 3b, 4c, and 5b). A relevant point is that while the initial amounts of isolated hydroxyls are similar in both samples (as is also the behavior of these species on interaction with toluene and subsequent reaction), H-bonded hydroxyls exist in rather different amounts, and the effect on them of toluene adsorption and UV irradiation is different. This can be related to observations that in the photoreaction tests the two specimens produce benzaldehyde with quite similar rates (both in the transient and steady-state regimes), while the production rate of CO_2 is rather different, not only in the final steady state but also in the initial stages which show activation/deactivation phenomena with different rates.

The first conclusion that can be drawn from these observations is that the formation of benzaldehyde is related to the interaction of toluene with the hydroxyls of isolated types, while the interaction with H-bonded hydroxyls can lead to complete oxidation of the organic substance. There is indeed a rationale to this: in areas with higher concentrations of OH groups, H-bonded hydroxyl forms may predominate and the interaction of the surface with the aromatic ring of the toluene molecule will be favored as a consequence of both the higher OH density (allowing multipoint interaction) and the more acidic character of those groups; zones with isolated OH groups, where those factors do not concur may favor a more localized interaction with mainly the methyl part of the hydrocarbon. A consequence will be that in the latter case the attack of surface radicals to the hydrocarbon during photoreaction will mainly affect side groups leading to benzaldehyde, while in the former adsorption mode it will be easier to directly attack the aromatic ring, the breakage of which may lead more easily to complete degradation.

Additional data can be fitted with the previously mentioned basic model of correlation between OH content and photocatalytic behavior. This is the case, for example, with the different ways in which toluene conversion varies with irradiation time. The conversion increase observed at the start of irradiation for P11h could be related to the generation of adsorption sites for oxygen, the other adsorbed species required for PCO; indeed the higher coverage with H-bonded OH groups observed for P11h may lead initially to a lower amount of titanium coordination vacancies at the surface needed for the generation of the first product of oxygen–photoelectron interactions (Ti-bonded O_2^- radicals). Those uncoordinated Ti sites would appear thus in sample P11h only after irradiation, which produces a significant loss of those hydroxyls (presumably as water) as shown in Fig. 4g. In the case of P11t, which shows a weaker hydroxyl population, photooxidation will proceed from the beginning, without such initial transient activation.

Figures 3c and 5c indicate that by irradiating the samples containing adsorbed toluene in the presence of oxygen, part of the IR band due to toluene-modified isolated hydroxyls disappears. This occurs without recovery of the initial isolated hydroxyl bands, indicating that the OH groups themselves, not just the modifying toluene molecules, have been consumed. One notes also the important decrease of the absorption in the 3500–3000 cm^{-1} range produced by irradiating P11h, but not P11t; this difference in H-bonded hydroxyls consumption (and also, although to a lesser extent, in the case of isolated ones) is clearly seen in the overall difference spectra shown in Figs. 3f and 5f. This difference may be related to the higher photoactivity shown by the P11h catalyst.

Since OH groups are important for photoactivity, one could relate these in principle to the conversion decrease observed for both samples (after an initial increase in the P11h case) in the first 50–100 min of photoreaction, which indicates that active sites are being eliminated or poisoned. If, as indicated by the FTIR spectra, hydroxyls are eliminated during toluene PCO, an important photocatalyst deactivation would be expected, ultimately leading to a stop in the reaction. The fact that total deactivation is not observed means that hydroxyls are being regenerated; furthermore, since sample P11h, which shows significant OH loss, suffers a smaller deactivation, it seems that hydroxyl regeneration is more efficient. A process for hydroxyl regeneration is the dissociation of water, which is present as added vapor while the material is irradiated in the photoreaction tests. The water dissociation process requires the presence of pairs of sites: one with acid character (low coordination titanium cations) to bind initially the water molecule and the other one with basic characteristics (exposed bridging oxygens) to accept the proton. The pairs should be placed at an appropriate distance if one wants to favor both water adsorption and the maintenance of a certain interaction between the resulting hydroxyls which may help in the process (23). This cooperative effect of acid and basic sites can be

obtained if the surface possesses an appropriate structural arrangement at the atomic scale. The presence of the broad band centered at 3100 cm^{-1} in the FTIR spectra might be taken as an indication of such water dissociation sites in anatase. Therefore, for P11t, whose surface is characterized by a smaller contribution of interacting hydroxyl groups, the rate of rehydroxylation may be lower, thus explaining the faster deactivation and lower steady-state conversion rate in comparison to sample P11h.

With all the previous arguments in mind, one main difference between both types of samples, with different photoactivities, lies in their different capability to initially possess, and especially to regenerate in the presence of water vapor during photoreaction, the hydroxyl groups which are fundamental for the activity. In the final steady-state stage, when the number of active sites for toluene oxidation no longer changes, this number is higher for sample P11h, leading to a higher value of total toluene conversion. The reason for this difference, in samples having the same BET area and crystallite size, is not yet clear, but it may be related to the different degrees of perfection of the (nano)crystals. The formation of these by calcination at high temperature in the P11t sample will lead probably to more perfect crystalline surfaces, with a higher proportion of flat crystal faces, while sample P11h, crystallized under hydrothermal conditions, may keep more surface irregularities (kinks, steps, etc.) stabilized during the synthesis as a consequence of the high concentration of ligand molecules (water and ethanol) and which in the final photocatalyst will constitute more active sites for low-temperature water dissociation. Thus one direction for photocatalyst improvement may consist in devising preparation methods which increase the amount of these surface irregularities while allowing them to remain stable and not readily poisoned by partial oxidation products during the photoreaction.

5. CONCLUSIONS

The treatment conditions used for the crystallization of an amorphous TiO_2 precursor not only influenced the anatase crystal size but also other anatase properties (such as the surface hydroxylation) that determine the photocatalytic properties of this catalyst. With respect to the thermal treatment used for the preparation of P11t, the hydrothermal treatment used for P11h induces a higher photoactivity for toluene degradation, together with a higher hydroxyl content under vacuum conditions.

As indicated by FTIR, though both samples present a similar number of isolated hydroxyl groups after outgassing at 295 K, the amount of H-bonded hydroxyls is more important for P11h. Both types of hydroxyl groups are lost during the photoreaction, which produces a decrease of toluene photoconversion that is more or less important dependent on the hydroxyl regeneration process. The photodegradation of toluene adsorbed on H-bonded hydroxyls, which can be regenerated by water dissociation when the reaction takes place in the presence of water vapor, justifies the higher steady conversion obtained using P11h as photocatalyst.

Benzaldehyde, a minor product of toluene oxidation, is produced by toluene adsorbed on isolated hydroxyls. In the absence of water vapor, it is retained by P11h more strongly than by P11t; however, water vapor helps benzaldehyde desorption.

ACKNOWLEDGMENTS

Financial support from ECSC (Contracts 7220-ED/093 and 7220-EB/004) is gratefully acknowledged. J.M.C. thanks C. A. M. for awarding a postdoctoral grant.

REFERENCES

1. Hoffmann, M. R., Martin, S. T., Choi, W., and Bahnemann, D. W., *Chem. Rev.* **95**, 69 (1995).
2. Mills, A., Davies, R. H., and Worsley, D., *Chem. Soc. Rev.* **93**, 417 (1993).
3. Fox, M. A., and Dulay, T., *Chem. Rev.* **93**, 341 (1993).
4. Maira, A. J., Soria, J., Augugliaro, V., and Loddo, V., *Chem. Biochem. Eng. Q.* **11**, 89 (1997).
5. Maira, A. J., Yeung, K. L, Chan, C. K., Porter, J. F., and Yue, P. L., *Stud. Surf. Sci. Catal.* **130**, 1949 (2000).
6. Cao, L., Huang, A., Spiess, F. J., and Suib, S. L., *J. Catal.* **188**, 48 (1999).
7. Maira, A. J., Yeung, K. L., Yan, C. Y., Yue, P. L., and Chan, C. K., *J. Catal.* **192**, 185 (2000).
8. Maira, A. J., Yeung, K. L., Soria, J., Coronado, J. M., Belver, C., Lee, C. Y., and Augugliaro, V., *Appl. Cat. B. Environ.* **29**, 327 (2001).
9. Xu, N., Shi, Z., Fan, Y., Dong, J., Shi, J., and Hu, M. Z.-C., *Ind. Eng. Chem. Res.* **38**, 373 (1999).
10. Anpo, M., Shima, T., Kodama, S., and Yutaka, K., *J. Phys. Chem.* **91**, 4305 (1987).
11. Augugliaro, V., Palmisano, L., Scalfani, A., Minero, C., and Pelizzetti, E., *Toxicol. Environ. Chem.* **16**, 89 (1988).
12. Okamoto, K., Yamamoto, Y., Tanaka, H., Tanaka, M., and Itaya, A., *Bull. Chem. Soc. Jpn.* **58**, 2015 (1985).
13. Morterra, C., *J. Chem. Soc., Faraday Trans.* **84**, 1617 (1988).
14. Cerrato, G., Marchese, L., and Morterra, C., *Appl. Surface Sci.* **70/71**, 200 (1993).
15. Kanaka, K., and White, J. M., *J. Phys. Chem.* **86**, 4708 (1982).
16. Primet, M., Pichat, P., and Mathieu, M.-V., *J. Phys. Chem.* **75**, 1216 (1971).
17. Nagao, M., and Suda, Y., *Langmuir* **5**, 42 (1989).
18. Cao, L., Gao, Z., Suib, S. L., Obee, T. N., Hay, S. O., and Freihaut, J. D., *J. Catal.* **196**, 253 (2000).
19. Méndez-Román, R., and Cardona-Martínez, N., *Catal. Today* **40**, 353 (1998).
20. Martra, G., Coluccia, S., Marchese, L., Augugliaro, V., Loddo, V., Palmisano, L., and Schiavello, M., *Catal. Today* **53**, 695 (1999).
21. Martra, G., *Appl. Catal. A: General* **200**, 275 (2000).
22. Coronado, J. M., Maira, A. J., Conesa, J. C., Augugliaro, V., and Soria, J., *Langmuir*, doi: 10.1021/LA0101531.
23. Henderson, M. A., *Langmuir* **12**, 5093 (1996).